K. M. Burson, M. Heyde, H.-J. Freund

LOOKING INTO THE STRUCTURE OF GLASS BY DESIGNING A NEW 2D MATERIAL

ABSTRACT

Determining the structure of amorphous materials used to be challenging due to the complexity of this material class. Here we review structural studies of bulk and two-dimensional amorphous silica, focusing on the recent discovery of a new 2D amorphous material. For the first time a clear image of an amorphous network structure has been obtained by using scanning tunneling and atomic force microscopy, which allowed for the derivation of atomic sites and a detailed analysis of real space coordinates. We discuss the benefits of these measurements on the newly developed thin silica bilayer film system and consider comparisons between two-dimensional structures and their three-dimensional bulk silica counterparts. Recent experiments which establish 2D amorphous silica as a candidate for an insulating material with application in two-dimensional nanoelectronics are also discussed.

INTRODUCTION

Silica is one of earth's most abundant minerals, accounting for approximately 60% of all oxides in the earth's crust by weight. Silicate glasses are the most important materials for the glass industry[1] and polymorphs of silica are used widely in applications ranging from supports for catalysis to microelectronics to optical fibers to flow agents in powdered foods. As a result of silica's physical, chemical, and geochemical importance, it has been extensively studied; in fact, structural studies of silica glass have been actively pursued for more than eighty years.[2] Experimental efforts have been dominated by X-ray and neutron diffraction studies, while theoretical investigations have primarily employed molecular dynamics simulations and Monte Carlo techniques. More recent experimental efforts have utilized scanning probe microscopy. Due to the complexity of the glass structure, and to commercial demands for specially tailored glassy materials,[1] many questions remain open concerning the atomic structure of amorphous silica and the nature of the glass transition. Recent studies on two-dimensional model silica systems provide detailed structural characterizations of silica that directly address some of these questions.

Dr. Kristen M. Burson#
Dr. Markus Heyde*
Prof. Dr. Hans-Joachim Freund
Fritz-Haber-Institut der Max-Planck-Gesellschaft
Faradayweg 4-6, 14195 Berlin, Germany
* Electronic mail: heyde@fhi-berlin.mpg.de
# Current Address: Hamilton College, Clinton, NY, USA

Two-dimensional materials have captured the scientific imagination as 2D materials often lead to new and unexpected materials properties that are distinct from their bulk counterparts. In many cases the bulk properties of the parent materials are well established and inform an understanding of the unique properties of the 2D material. Although 2D amorphous silica might reveal new properties in comparison to bulk materials, given that many unknowns exist surrounding the structure of bulk glass, it is worth comparing its structure to bulk structural studies in order to gain insights into the nature of bulk glass materials. Instead of using bulk properties to understand the nanoscale, we can use this nanomaterial to understand bulk properties of glass. Here we briefly review key historical developments in understanding the structure of silica glass and review recent results from atomic-resolution structural studies of two-dimensional silica glass. Results from two-dimensional model glasses are discussed in comparison with studies of bulk silica, highlighting the key advantages (and limitations) of using lower-dimensional model systems as a tool for understanding their bulk counterparts.

HISTORICAL DEVELOPMENT OF THE STUDY OF SILICA: DIFFRACTION STUDIES AND THE RANDOM NETWORK THEORY

Early experimental studies of silica used X-ray diffraction and neutron diffraction to infer the atomic structure. Figure 1a, shows Max von Laue at a meeting of scientists in 1912 in Munich, Germany. Two years later he would win the Nobel prize for his "discovery of the diffraction of X-rays by crystals." Since the initial discovery, diffraction techniques have been employed to deduce the atomic structure of a variety of crystalline materials with great success. Figures 1b and 1c show images of the X-ray diffraction patterns from crystalline α-quartz and silica glass collected using the original powder diffraction method of Debye and Scherrer.[3] The α-quartz diffraction pattern shows a sharp set of rings associated with the long range periodicity in atomic arrangements. Due to the presence of distinct peaks, clear assignment of interatomic distances and crystal structure can be established, while the silica in its amorphous state shows a diffuse set of rings in the diffraction pattern. The pair correlation function obtained from X-ray diffraction experiment shown in Figure 1d, reveals that peaks in the diffraction data get broader with increasing radial distance. Such line shapes must be interpreted with the aid of complex structural models and, even with thorough models, accurate interpretation can be difficult. Furthermore, because diffraction techniques average over large spatial areas of the bulk crystal, XRD and ND do not provide direct atomic position information, but rather a spatially averaged statistical measure of the relative distance between

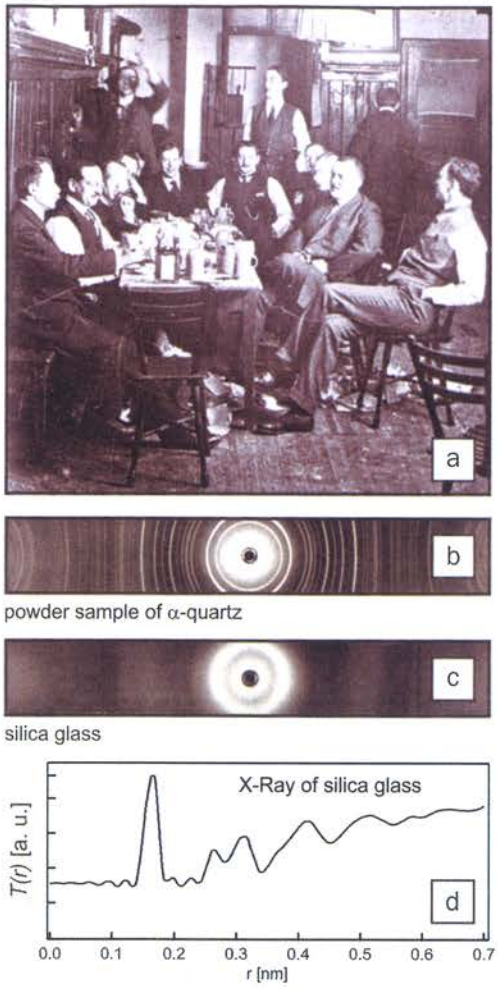

Fig. 1: (a) Max von Laue in Munich (at table on left) in 1912 with Paul Sophus Epstein (left near Laue) and Peter Paul Ewald (right side of table, second from the front) among other physicists (this photograph is a courtesy from the "Archiv der Max-Planck-Gesellschaft"), (b) X-ray diffraction patterns collected from powered α-quartz samples by the method of Debye and Scherrer show distinct ring peaks, while the X-ray diffraction pattern from bulk silica glass (c) shows only diffuse halos. (d) pair correlation function obtained from X-ray diffraction on a bulk silica glass.[3]

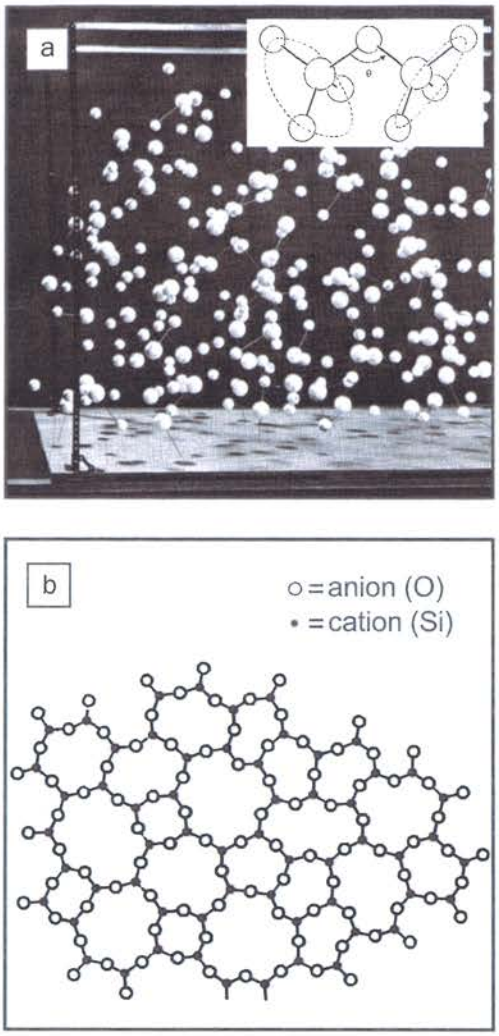

Fig. 2: Models for the atomic structure of glass. (a) an early three-dimensional model by Bell and Dean[5], (b) two-dimensional model presented by Zachariasen[6].

atoms of the same species. As such, the technique precludes atomic-scale structural determination for amorphous materials. Nonetheless, a number of useful descriptors of the glassy structure can be derived from XRD and ND studies including the Si-Si distance, O-O distance, and Si-O distance. Si-O-Si and O-Si-O bond angle distributions as well as bond torsion angles can also be established, although with greater uncertainty. Features at larger length scales, associated with network topology and longer range density fluctuations are much less well understood[4]; interpretation of data from these regimes requires detailed computer modelling and simulation.

DEVELOPMENT OF MODELS

Models of silica have necessarily been developed in conjunction with experimental studies of silica. The "random network theory" was developed in the seminal works of Zachariasen and Warren.[6, 7] The theory continues to shape the understanding of glassy structure in the modern era of glass research (although a competing 'crystallite theory' resulted in some debate, especially in the 1970s and 1980s). Zachariasen proposed that silica in both crystalline and amorphous forms is formed from corner sharing SiO_4 tetrahedral building blocks and that the differences between crystalline and amorphous forms stem from distinct arrangements of these building blocks. In the crystalline structure, bond angles are fixed and the tetrahedra are arranged periodically; in the amorphous structure, a random network forms with a greater variance in bond angle and aperiodic structure (the term 'random network' itself was used only later, by Warren,[7] to describe the structure that Zachariasen had published[6]). In 1966, Bell and Dean created a physical three-dimensional version of the random network model using steel wires and polystyrene spheres (Figure 2a).[5] Their goal was to establish a connection between precisely defined atomic models of silica and experimental structural data that was by nature statistical. By computing radial distribution functions from the model coordinates using X-ray form factors, Bell and Dean demonstrated a strong correlation between their ball and stick atomic model and existing X-ray diffraction data. A two-dimensional version of the random network model was included in Zachariasen's original paper and is shown in Figure 2b.[6] In the simplified presentation, SiO_3 building blocks are arranged in a planar structure and a network of different rings sizes can be

observed. Bell and Dean's application of random network theory to a three-dimensional model was a key step for assessing the validity of the theory against available experimental data. As highlighted by the work of Bell and Dean, the accuracy of models based on random network theory is evaluated by assessing the relationship between pair correlation functions from the model networks and spectra from XRD and ND data. Recent computer models and simulations using reverse Monte Carlo,[8] molecular dynamics simulations,[9] and density functional theory[10, 11] capture more precise atomic arrangements, but necessitate the same approaches for comparison with experiment. Diffraction studies average over the bulk of the crystal and therefore can never give local atomic structure data of amorphous materials; this limits connections between theory and experiment to one-dimensional comparisons that do not capture the full detail of the three-dimensional structures. More precise experimental data is needed on the atomic structure of glass in order to better address the validity of atomic models of silica.

FROM 3D SILICA TO 2D BILAYER SILICA

With the advent of atomic-resolution scanning probe microscopy (SPM) techniques, it became possible to acquire local structure data on a variety of complex surfaces.[15–18] Initial attempts to resolve the surface structure of amorphous silica with atomic force microscopy,[12] shown in Figure 3a, were difficult to interpret due to the roughness of the sample surface. Interactions between multiple tip atoms and rough, complex sample surfaces inhibit clear atomic resolution, as shown schematically in Figure 4a and described in reference[19]. Best resolution can be achieved when the interaction between the front tip atom and the sample is the primary interaction responsible for image contrast (shown in Figure 4b). Full atomic-resolution of the glass structure was attained only with the development of a two-dimensional bilayer silica film, ideally suited for studies utilizing modern surface science techniques. Observations of the silica structure were achieved with SPM[20–22] and independently verified by a transmission electron microscopy study (TEM).[23, 24] The atomically flat surface of the two-dimensional model system enabled clearly interpretable, atomic-resolution imaging. Figure 3b shows a scanning tunneling microscopy image of an amorphous bilayer silica film with individual silicon

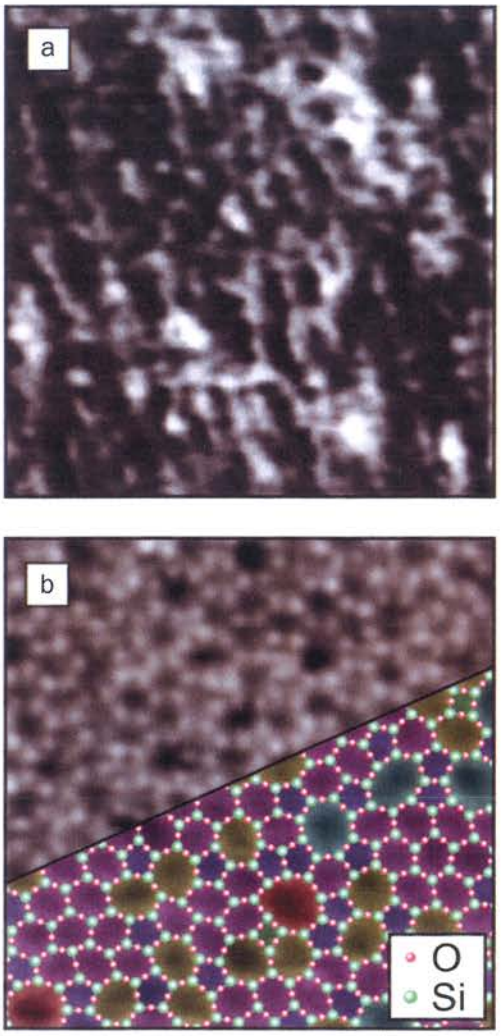

Fig. 3: Atomic force microscopy of silica structures (a) bulk silica[12] and (b) two-dimensional silica bilayer[13]. An atomic model is superimposed on the lower half of image (b) indicating ring sizes by color as well as atomic positions of silicon (green spheres) and oxygen (red spheres) from the top silica plane. Both images show a scan frame of 7 nm × 7 nm.

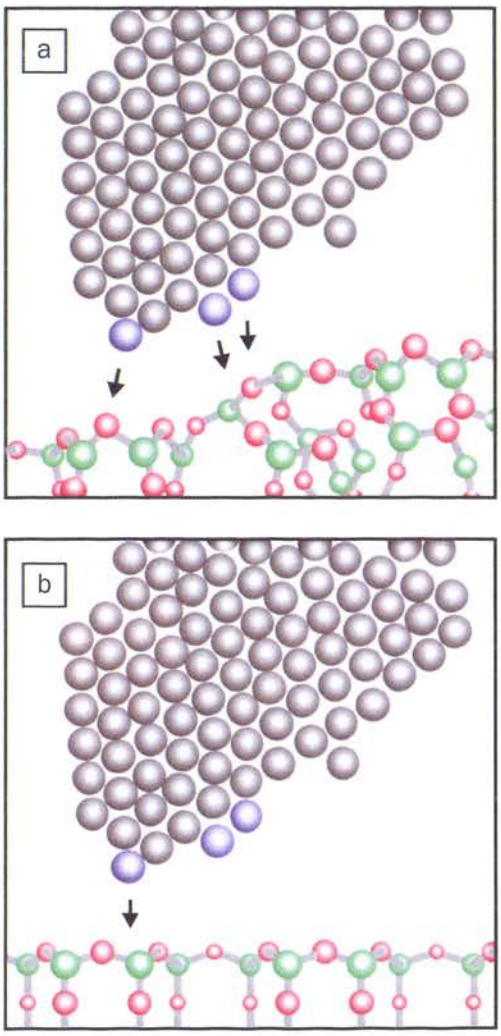

Fig. 4: Schematic diagram of tip-sample interactions for (a) a rough surface and (b) an atomically-flat surface.[14]

atoms clearly resolved. In general, either individual silicon atoms or individual oxygen atoms are resolved, depending on the local tip configuration.[21] Each silicon atom is bonded to three oxygen atoms in the plane and one oxygen bridging to the two silica planes; the structure was established by a combination of infrared spectroscopy (IRAS), density functional theory (DFT), and SPM[25] and a side view of the structure is shown schematically in Figure 4b. The 180° angle for the Si-O-Si in the silica bilayer between the top most and bottom layer is notable and deviates from the typically observed average angle of 144° for Si-O-Si structures (see Table 1). Nevertheless this angle agrees well with calculations predicting a flat potential for the Si-O-Si bond angle.[11] As in the model of Zachariasen, the SiO_4 tetrahedra serve as building blocks from which a network of different ring sizes is formed. Differences between building blocks for bulk and two-dimensional structures can be seen in Figure 5.

crystalline	STM_{oxygen}	$STM_{silicon}$	XRD	ND	ab initio	
Si-O [Å]	1.67 ± 0.08	1.66 ± 0.06	1.61	1.61	1.61-1.62	
O-O [Å]	2.71 ± 0.18	2.72 ± 0.11	2.63-2.65	2.63	2.62-2.65	
O-Si-O [°]	109.4 ± 8.1	110.1 ± 5.7	108.8-110.5	108.7-110.5	108.5-110.2	
Si-Si [Å]	3.12 ± 0.08	3.15 ± 0.11	3.06	3.06	3.07	
Si-O-Si [°]	139.9 ± 2.3	143.5 ± 1.2	143.7	143.6	144-148	
Si-Si-Si [°]	120.2 ± 6.3	119.5 ± 6.9				
vitreous	STM_{oxygen}	$STM_{silicon}$	XRD	ND	ab initio	Bell&Dean
Si-O [Å]	1.60 ± 0.09	1.61 ± 0.11	1.62	1.61 ± 0.05	1.61-1.63	1.59 ± 0.03
O-O [Å]	2.59 ± 0.21	2.65 ± 0.19	2.65	2.63 ± 0.09	2.63-2.67	2.60 ± 0.08
O-Si-O [°]	109.2 ± 10.9	109.4 ± 12.6	109.8	109.7 ± 4.5	109.3-109.5	109.4 ± 4.9
Si-Si [Å]	3.01 ± 0.12	3.07 ± 0.23	3.12	3.08 ± 0.11	3.03-3.12	3.11 ± 0.07
Si-O-Si [°]	140.5 ± 2.3	142.6 ± 2.7	144 (152)		143.4-152.2	154.2 ± 9.3
Si-Si-Si [°]	120.2 ± 14.7	118.8 ± 15.3				104.9 ± 17.8
Si-Si-Si [°]	119.9 ± 10.6	119.9 ± 13.2				

Table 1: Silica bond lengths and bond angles from STM images with oxygen and silicon contrast, XRD, ND, and ab initio calculations. This table has been adapted from reference[21] and the origin of these values is described therein in detail.

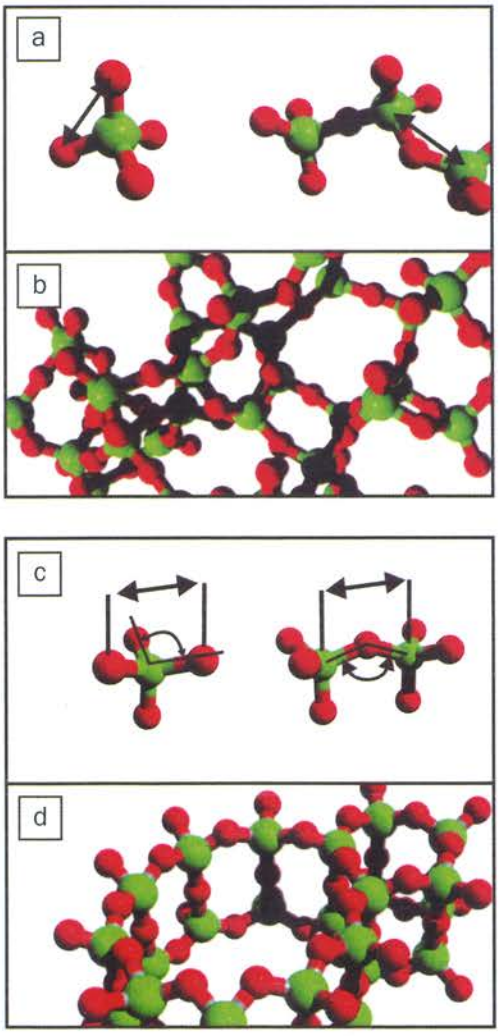

Fig. 5: (a) SiO_4 building block and (b) model structural arrangements for bulk structures. (c) SiO_4 building block and (d) model structural arrangements for silica bilayers.

The experimentally observed network in Figure 3b is, qualitatively, strikingly similar to the predictions of Zachariasen's random network theory shown in Figure 2b. The two-dimensional model silica structure is also quantitatively consistent with studies of bulk silica structure from XRD and ND.[21] Directly measured bond lengths and angles for both crystalline and vitreous phases of silica bilayer agree well with bond lengths and angles determined from XRD and ND for bulk samples of crystalline and vitreous silica. Additionally, pair distances are calculated for each species individually based on the real space atomic position data for silicon and oxygen atoms.[26] Scaling each element-specific pair correlation function by its sensitivity factor for XRD and ND facilitates direct comparison with XRD and ND measurements of bulk silica. These comparisons show strong agreement between the two-dimensional data and the bulk data, indicating that the structural properties of the two-dimensional system reproduce those of bulk silica samples.

RING STATISTICS AND NEIGHBORHOODS

Silica bilayers present a distinct advantage over bulk studies in that they allow for more detailed structural assessment. The work discussed in the previous section reduced the two-dimensional atomic position data to a one-dimensional pair distance histogram (PDH) in order to directly compare with bulk XRD and ND. If instead the full two-dimensional image is considered, the network of ring sizes visible in the scanning probe microscopy data allows for quantization of ring sizes and distributions, ring neighborhoods, boundary structures, and short, mid, and long-range order. This level of detail is precluded by the spatially averaged data of diffraction techniques.

Rings are composed from the SiO_4 tetrahedral building blocks, with ring size defined as the number of silicon atoms present in the ring. A network of different ring sizes is clearly visible in

the experimental scanning probe microscopy images of the silica bilayer. The flexibility and ability to form different ring sizes is related to the flat potential of the Si-O-Si angle,[11] which gives rise to a variety of different structural elements in the amorphous silica bilayer. Figure 6a displays a theoretical calculation of ring sizes distributions by Shackelford and Davila which predict ring sizes distributions for bulk silica glass at a wide range of pressures from molecular dynamics simulations.[27] The results suggest a normal distribution as the probability distribution function for glasses at high pressures. In another study, Shackelford studied a two-dimensional triangular network and concluded that the continuous random network had a log-normal probability distribution function.[28] Ring statistics counted directly from images of silica bilayer samples confirm this prediction. Figure 6b shows the ring statistics for the silica bilayer. There are more five-membered rings than seven-membered rings and more eight-membered rings than four-membered rings. Nine-membered and larger rings sizes are rarely observed. The asymmetric distribution is fit well by a log-normal distribution (indicated by the red dotted line) in agreement with the early predictions of Shackelford.

Figure 7a demonstrates the limits of diffraction techniques. Correlation functions obtained from XRD (bottom) and ND (top) data are shown in comparison to those calculated with a relaxed version[30] of the Bell and Dean random network theory model.[31] From these fittings Si-O-Si bond angle distributions may be determined and the prediction of the basic tetrahedral SiO_4 building block corroborated, but data for structural features associated with network topology is difficult to interpret. In contrast, the network topology within the bilayer silica can be directly addressed by looking at ring neighborhoods. Looking at the top plane of the bilayer silica reveals the basic SiO_3 building blocks with three connections in the 2D plane. Individual rings are viewed as larger building units, composed from arrangements of the smaller SiO_3 building blocks, which tile the two-dimensional film. Büchner et al. analyzed ring neighborhoods by considering typical ring-size combinations for ring triplets and ring-size distributions around a central ring of a given size.[32] Ring triplets are defined as sets of three silica rings that share a common central vertex; an example of a 567 triplet is shown in Figure 6b. The most common ring triplets observed in the bilayer in order of prevalence are 567, 667, 566, 568, and 666 combinations. Ring triplet combinations

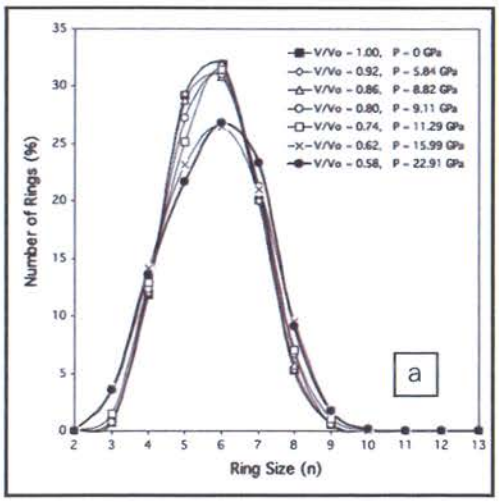

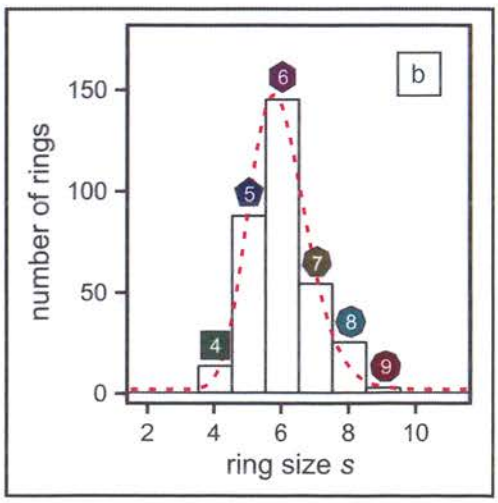

Fig. 6: Ring statistics for (a) bulk silica from molecular dynamics simulations[27] and (b) two-dimensional bilayer silica from scanning probe microscopy data[29]

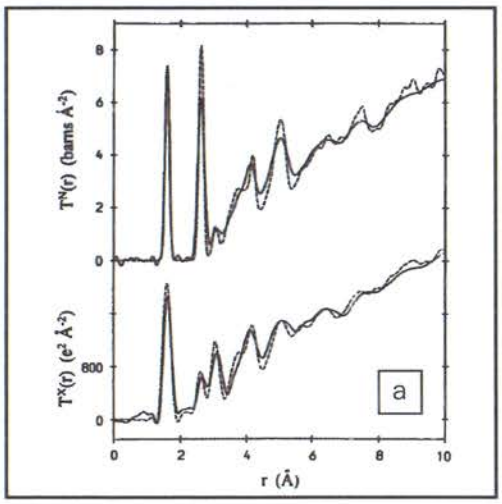

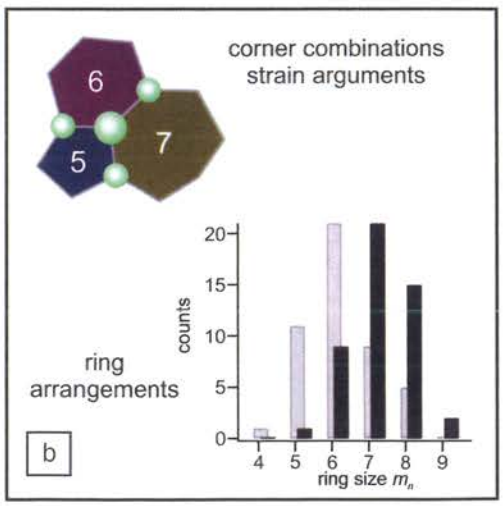

Fig. 7: (a) Neutron and X-ray diffraction data are shown by solids lines along with pair correlation functions based on theoretical models (dashed lines)[30] (b) Ring neighborhood analysis from Buchner et al. A schematic example of a ring triplet combination is shown in the upper left. A histogram of ring sizes for nearest neighbor rings surrounding a central 4-membered ring are shown as black bars with the log-normally distributed individual ring statistics for the entire system shown in gray.[32]

are influenced both by the relative probability of the individual ring sizes and by local geometry constraints imposed by the two-dimensional plane. Ring-size distributions around a given ring depend on the size of the central ring. For example, Figure 7b shows that ring-size distributions around 4-membered rings are shifted to larger ring sizes with respect to the uncorrelated individual ring-size distribution represented in Figure 6b. Comparably, larger sized central rings tend to be surrounded by smaller ring sizes. These neighborhood trends reveal the important role of geometric constraints in the spatial distribution of different ring sizes.

BOUNDARIES AND INTERFACES

The nature of the crystalline to glass transition is a subject of some debate. Establishing local structures at crystalline-vitreous interfaces may elucidate the ways in which materials transition from crystalline to vitreous structures. Relatedly, domain boundaries are structural defects which introduce diverse ring sizes and structural defects into otherwise crystalline domains. Figure 8a shows a predicted domain boundary structure at the surface of bulk α-quartz, based on He-atom scattering experiments, atomic force microscopy, and density functional theory.[33] The boundary is a Dauphiné twin boundary composed of six-membered rings. In 2D bilayer silica, multiple boundary types have been identified within crystalline domains of bilayer silica. The most common boundary structures are tilt boundaries consisting of 5- and 7-membered rings and antiphase domain boundaries consisting of 5- and 8-membered rings (with two 5-membered rings for every 8-membered rings). Examples of both 57 and 558 type domain boundaries are evident in Figure 8b. Domain boundaries are sometimes considered to be amorphous regions between crystalline domains. Statistics of the different ring sizes introduced into the crystalline structure by domain boundaries and defect structures show similarities to the relative prevalence of different ring sizes in the amorphous phase. However, the domain boundaries observed in bilayer silica also exhibit periodicity and order that distinguish their structure from that of amorphous phases.[34] Thus as it pertains to the glass transition, it is hard to reconcile glass transition models which assume amorphous structures to arise from highly defected crystalline ones with the observed domain boundaries structures in silica bilayers.

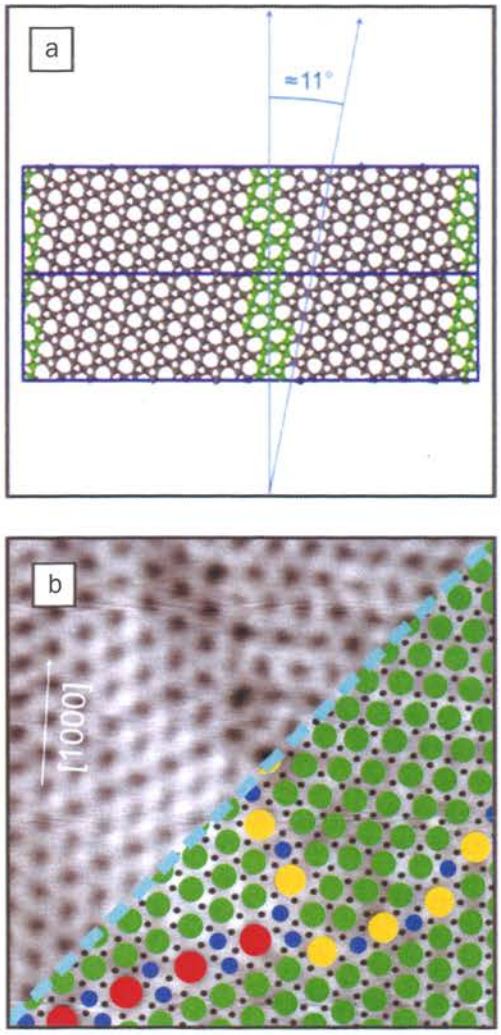

Fig. 8: (a) Dauphiné twin boundary composed of six-membered rings predicted for bulk silica surfaces based on He-atom scattering experiments, atomic force microscopy, and density functional theory.[33] (b) 57 tilt boundaries and 558 antiphase domain boundaries identified in crystalline bilayer silica resolved by STM with a scan frame of 7.4 nm × 7.4 nm.[34] An atomic model indicating silicon atomic sites (black dots) and ring sizes (colored circles) is superimposed on the lower half of the image.

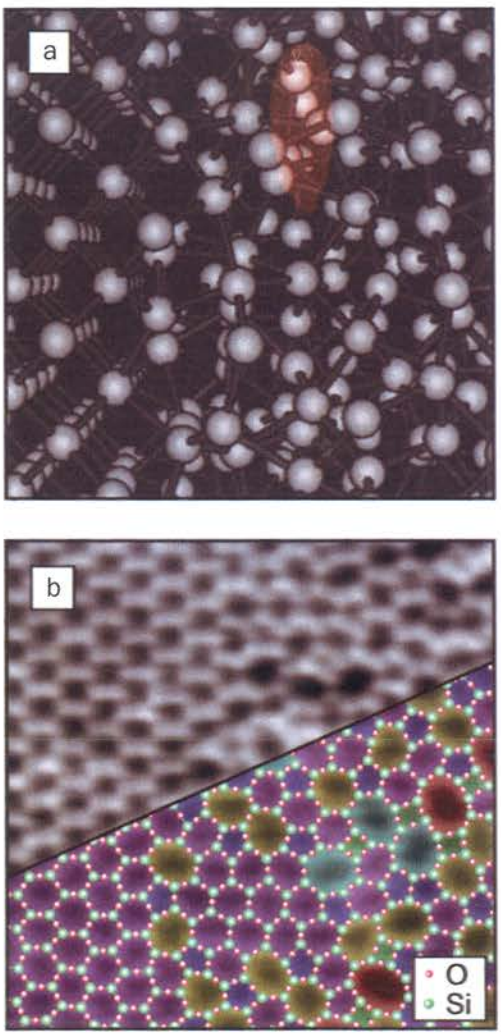

Fig. 9: (a) A computer-generated picture of the crystalline/amorphous silicon interface model.[35] (b) Atomically resolved STM image of the crystalline-vitreous interface in the silica film with a scan frame of of 7 nm × 7 nm.[13]

are influenced both by the relative probability of the individual ring sizes and by local geometry constraints imposed by the two-dimensional plane. Ring-size distributions around a given ring depend on the size of the central ring. For example, Figure 7b shows that ring-size distributions around 4-membered rings are shifted to larger ring sizes with respect to the uncorrelated individual ring-size distribution represented in Figure 6b. Comparably, larger sized central rings tend to be surrounded by smaller ring sizes. These neighborhood trends reveal the important role of geometric constraints in the spatial distribution of different ring sizes.

BOUNDARIES AND INTERFACES

The nature of the crystalline to glass transition is a subject of some debate. Establishing local structures at crystalline-vitreous interfaces may elucidate the ways in which materials transition from crystalline to vitreous structures. Relatedly, domain boundaries are structural defects which introduce diverse ring sizes and structural defects into otherwise crystalline domains. Figure 8a shows a predicted domain boundary structure at the surface of bulk α-quartz, based on He-atom scattering experiments, atomic force microscopy, and density functional theory.[33] The boundary is a Dauphiné twin boundary composed of six-membered rings. In 2D bilayer silica, multiple boundary types have been identified within crystalline domains of bilayer silica. The most common boundary structures are tilt boundaries consisting of 5- and 7-membered rings and antiphase domain boundaries consisting of 5- and 8-membered rings (with two 5-membered rings for every 8-membered rings). Examples of both 57 and 558 type domain boundaries are evident in Figure 8b. Domain boundaries are sometimes considered to be amorphous regions between crystalline domains. Statistics of the different ring sizes introduced into the crystalline structure by domain boundaries and defect structures show similarities to the relative prevalence of different ring sizes in the amorphous phase. However, the domain boundaries observed in bilayer silica also exhibit periodicity and order that distinguish their structure from that of amorphous phases.[34] Thus as it pertains to the glass transition, it is hard to reconcile glass transition models which assume amorphous structures to arise from highly defected crystalline ones with the observed domain boundaries structures in silica bilayers.

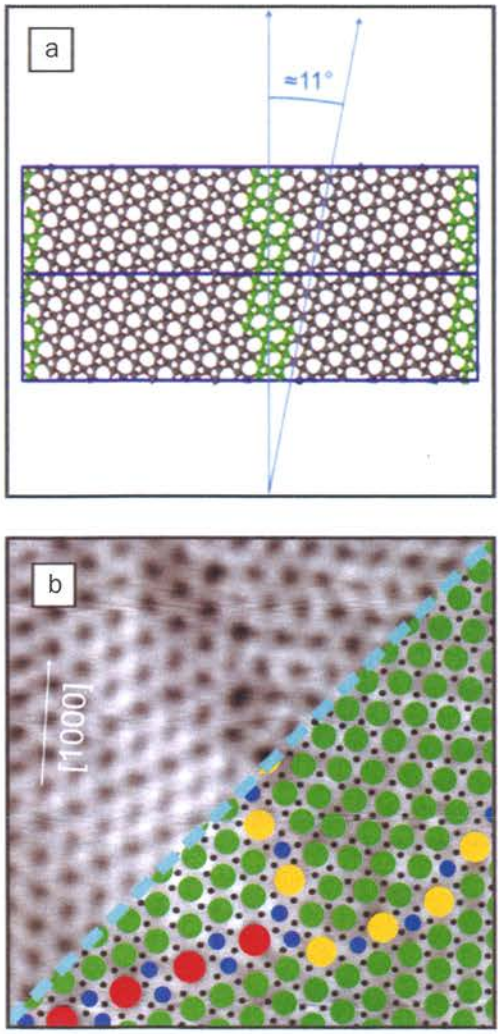

Fig. 8: (a) Dauphiné twin boundary composed of six-membered rings predicted for bulk silica surfaces based on He-atom scattering experiments, atomic force microscopy, and density functional theory.[33] (b) 57 tilt boundaries and 558 antiphase domain boundaries identified in crystalline bilayer silica resolved by STM with a scan frame of 7.4 nm × 7.4 nm.[34] An atomic model indicating silicon atomic sites (black dots) and ring sizes (colored circles) is superimposed on the lower half of the image.

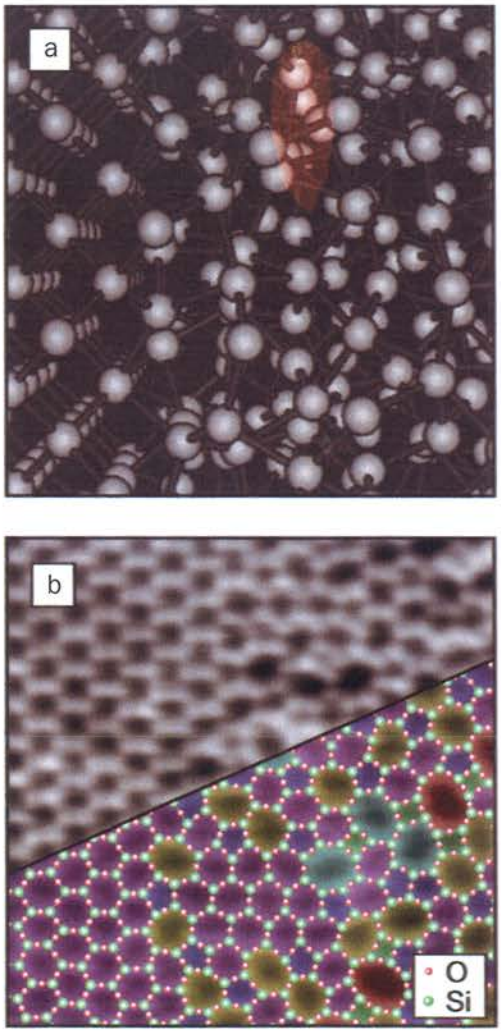

Fig. 9: (a) A computer-generated picture of the crystalline/amorphous silicon interface model.[35] (b) Atomically resolved STM image of the crystalline-vitreous interface in the silica film with a scan frame of of 7 nm × 7 nm.[13]

Interface structures of spatial transitions from crystalline to vitreous structures provide insight relevant to understanding the glass transition. Figure 9a shows a computer generated model of the crystalline-vitreous interface in silicon generated using a simulated anneal method. Using a temperature differential to stabilize the phases on opposite sides of the interface in the 512 atom simulation produced a sharp interface with an interfacial region of only 3Å.[35] An experimental scanning probe microscopy image of the interface in the two-dimensional silica bilayer is shown in Figure 9b.[13] The degree of crystallinity was analyzed as a function of lateral position across the interface. Based on changes in the crystallinity, the crystalline-vitreous spatial transition is found to be continuous with an interfacial region on the order of 1.6-2.4 nm.[13, 36]

RANDOM NETWORKS AT DIFFERENT LENGTH SCALES

To this point, we have focused on the atomic scale amorphous silica network. However, random network structures are observed for structures at a variety of length scales from atomic scale glassy structures to molecular networks to macroscale bubbles. Some of the structural features analyzed for bilayer silica are reproduced in other two-dimensional random networks at different length scales.[37] Bubble rafts were used by Bragg and Nye[38] as an example of crystalline structures and grain boundaries. We developed amorphous bubble raft films and crystalline to amorphous bubble raft transitions, as shown in Figure 10. The bubble rafts show strong similarities to silica bilayers in both the ring statistics and the continuous transition behavior at the crystalline-amorphous interface.[36] The similarity of structural features between the nanoscale and millimeter scale amorphous network formers points to possible universal features of two-dimensional network formers. For both bubble rafts and silica, it is important to assess the extent to which the observed structures are unique to two-dimensions and to what extent the insights gained from structural assessments of two-dimensional random networks are transferrable to bulk amorphous structures.

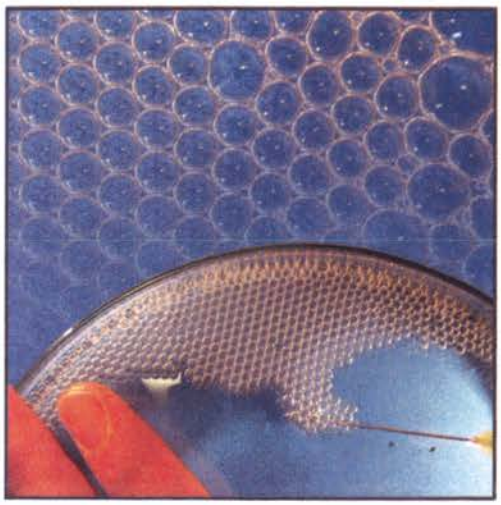

Fig. 10: Crystalline-amorphous interface for a bubble raft (top) and preparation technique for the bubble raft (bottom)

LIMITS OF THE 2D SILICA MODEL

2D analogs reproduce many of the characteristics observed in their 3D counterparts: silica bond angles and atomic neighbor distances show strong agreement with XRD and ND results. Domain boundaries, interfaces, and ring size distributions have been investigated for both 2D and bulk silica. In some cases no analogous experimental data on bulk silica exists for comparison with the bilayer silica results. Ring neighborhoods, for example, are not addressable by diffraction measurements of bulk silica, but can be directly assessed with atomic resolution real-space images from the silica bilayer. However, one should be cautious when applying results from silica bilayers, a two-dimensional model system studied extensively in ultra-high vacuum environments, to applications with bulk silica. A growing interest in building nanoelectronics from the bottom up has led to rapid development of a class of two-dimensional materials for nanotechnology. Isolated atomic planes can also be reassembled into designer heterostructures made layer by layer in a precisely chosen sequence (often referred to as "van der Waals" heterostructures). These 2D materials often exhibit characteristics distinctly different redundant from their bulk counterparts.[39] 2D bilayer silica is no exception to this trend, exhibiting some characteristics that are particular to the 2D structure. For example, the individual ring statistics in two-dimensions are distinct from those predicted for three-dimensional structures[27] due to the geometric constraints of filling a two-dimensional space.[32] While a two-dimensional top view of the silica bilayer reveals a network of different ring sizes consistent with the predictions of Zachariasen[6] and Shackelford,[28] if the third dimension connecting the two atomic planes in the silica bilayer is considered, an abundance of 4-membered rings can also be identified; thus in this case 4-membered rings are over-represented with respect to bulk silica. Given that some properties are unique to the silica bilayer structure, bilayer silica should not only be considered as an analog to bulk silica, but also be explored for its utility as a 2D material for nanoelectronic heterostructure devices. Because silica is an insulating material used ubiquitously in the semiconductor industry, bilayer silica is a promising candidate for use as a gate dielectric material in nanoelectronic devices. Yet, many of the device structures currently employed for the study of two-dimensional nanoelectronics are developed, at least in part, under ambient conditions. The idealized conditions of ultra-high vacuum experiments are quite distinct from the environments utilized for nanotechnology device development and for many industrial and technological applications of silica. In order to address the gap between current studies and real world applications and in order to add bilayer silica to the library of two-dimensional materials for nanoelectronic heterostructures, studies of bilayer silica under ambient conditions must be pursued.

MOVING TOWARDS APPLICATIONS

To date, most of the research on silica bilayers has been performed in idealized ultra-high vacuum environments. These conditions provide a high degree of experimental control which enables unambiguous structural assessment. Yet real world applications of silica and its derivatives demand higher pres-

sures and temperatures and occur in varied environmental conditions. Recent research on silica bilayers beyond ultra-high vacuum addresses these practical considerations by bridging the gap between UHV and ambient pressure.

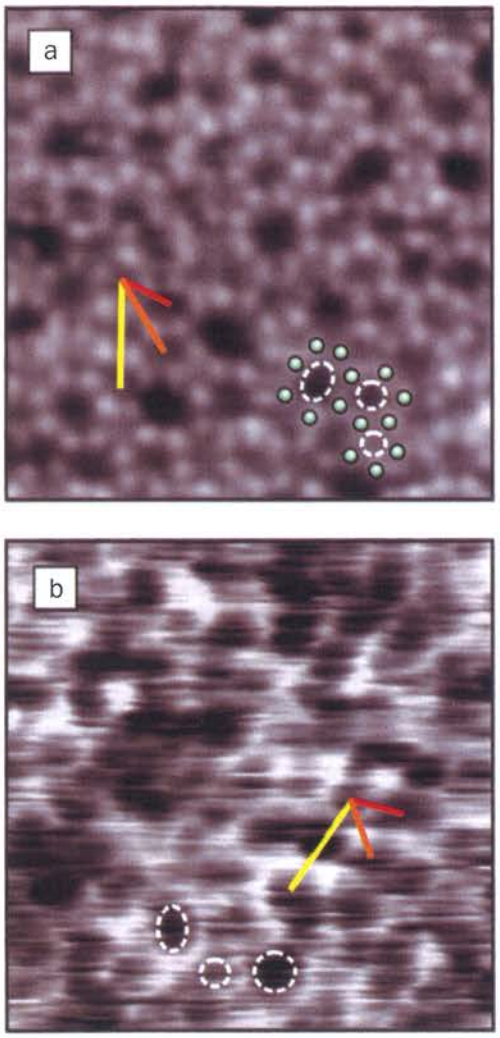

Fig. 11: (a) An amorphous silica bilayer film with atomic resolution of silicon atoms by STM in (a) and ring resolution by liquid-AFM in (b). Both images have a scan frame of 5 nm × 5 nm. Red, orange, and yellow measurement bars show examples of ring center-center distances for the first three families of ring neighbors identified in the amorphous silica bilayer. Several individual rings are marked in each image[44].

In order to bridge the gap between UHV and ambient conditions, the structure of silica has been investigated with high-resolution liquid atomic force microscopy. Silica films are grown in UHV and subsequently transferred to the liquid environment (400 mM NaCl solution). Figure 10a shows images of the bilayer silica structure attained with ultra-high vacuum STM (11a) and high resolution liquid-AFM (11b).[14] The low-temperature UHV STM images exhibit atomic resolution of the silica structure while the room temperature liquid-AFM images exhibit ring resolution. The structures appear remarkably similar and quantitative assessment from pair distribution functions of the ring center positions confirms the qualitative agreement. These results show that the silica film is structurally robust against ambient conditions; this result is consistent with the conclusions of a previous study which found the silica bilayer film to be exceptionally stable against hydroxylation.[40] Using thermal desorption spectroscopy and scanning tunneling microscopy under vacuum conditions, only small amounts of silanols (Si–OH) were observed. In contrast, many UHV surface structures are not stable under ambient conditions due to unsaturated bonds.[41, 42] The stability of the silica bilayer makes it an optimal playground to test the resolution of liquid AFM as the amorphous structure circumvents the common challenge of distinguishing between true atomic resolution and lattice resolution.[43] Furthermore, establishing the stability of the silica bilayer under ambient conditions opens the door to future device applications.

Silica bilayers are an ideal candidate material for inclusion in two-dimensional nanoelectronic heterostructures due to their insulating character[44] and high degree of structural integrity under ambient conditions. Novel nanoelectronic heterostructure devices are designed with tailored properties by bottom-up production which combines two-dimensional insulating, semi-conducting, and conducting materials. Numerous options exist for two-dimensional semiconductors, yet to date hexagonal boron nitride is the most widely used two-dimensional insulator. Silica bilayers are wide band-gap insulators with band gaps on the order of 6.5-7.3 eV[45, 46] and provide a two-dimensional analog of the SiO_x insulating layer used in the semi-conductor industry. In order to use bilayer silica for nanoelectronic devices, transfer of the bilayer from the growth substrate is necessary. Silica bilayers are grown on Ru(0001) in vacuum and subsequently moved to ambient conditions.[47] The silica bilayer has been successfully transferred to a new Pt(111) substrate via polymer assisted mechanical exfoliation. The transferred sample is heated to remove polymer residue and the structural integrity of the silica film is maintained throughout the process. With this achievement, silica has been added to the toolbox of two-dimensional materials for nanoelectronics, bridging the gap between fundamental structural studies and technological applications.

CONCLUSION

To conclude, this work has significantly enhanced our understanding of the prototype amorphous solid, silica, through the use of high-resolution imaging and spectroscopy on a two-dimensional amorphous silica bilayer. Scanning probe microscopy allowed for direct assessment of structural features on multiple length scales which were previously inaccessible in structural studies of silica due to the spatial resolution limits and spatially averaged nature of diffraction techniques. Silica bilayers are used not only to inform a structural understanding of their bulk counterpart, but also to assess other two-dimensional amorphous materials from the nanoscale to the macroscale. Silica bilayer structures have been shown, as well, to have utility in their own right as they are structurally robust against environmental conditions and can be transferred for use in tailored nanoelectronic device structures.

We have shown in this review that the silica network is a unique system for studying amorphous and crystalline structural elements. Currently, we are working on growth of other film systems that might also provide similar structural modifications. Promising candidates in that direction are germania and bo-

rate films. Furthermore, additional studies of the silica bilayer should be pursued to extend the characterization of this unique material. Mapping band structure differences between crystalline and vitreous domains, addressing vibrational and phonon modes, and exploring atomic scale dynamics with high-speed, variable temperature scanning probe microscopy techniques would provide valuable new insight.

ACKNOWLEDGEMENTS

The support by the German Science Foundation through CRC 1109 "Understanding of Metal Oxide/Water Systems at the Molecular Scale: Structural Evolution, Interfaces, and Dissolution" is gratefully acknowledged. K.M.B. thanks the Alexander von Humboldt foundation for funding. We thank J. Sauer and his group for the long standing collaboration on this project.

REFERENCES

[1] J.C. Mauro, C.S. Philip, D.J. Vaughn, and M.S. Pambianchi, *Int. J. Appl. Glass Sci.* **5**, 2 (2014).

[2] A.C. Wright and M.F. Thorpe, *Phys. Status Solidi B* **250**, 931 (2013).

[3] H.S. Peiser, H.P. Rooksby, and A.J.C. Wilson, editors , *X-Ray Diffraction by Polycrystalline Materials* (Institute of Physics, London, 1955).

[4] A.C. Wright, *J. Non-Cryst. Solids* **179**, 84 (1994).

[5] R.J. Bell and P. Dean, *Nature* **212**, 1354 (1966).

[6] W.H. Zachariasen, *J. Am. Chem. Soc.* **54**, 3841 (1932).

[7] B.E. Warren, Z. *Für Krist. - Cryst. Mater.* **86**, 349 (1933).

[8] X. Yuan and A.N. Cormack, *J. Non-Cryst. Solids* **319**, 31 (2003).

[9] D.A. Keen and M.T. Dove, *J. Phys. Condens. Matter* **11**, 9263 (1999).

[10] M.R. Bär and J. Sauer, *Chem. Phys. Lett.* **226**, 405 (1994).

[11] J. Sauer and B. Ŀurawski, *Chem. Phys. Lett.* **65**, 587 (1979).

[12] W. Raberg and K. Wandelt, *Appl. Phys. -Mater. Sci. Process.* **66**, S1143 (1998).

[13] L. Lichtenstein, M. Heyde, and H.-J. Freund, *Phys. Rev. Lett.* **109**, 106101 (2012).

[14] K.M. Burson, L. Gura, B. Kell, C. Büchner, A.L. Lewandowski, M. Heyde, and H.-J. Freund, *Appl. Phys. Lett.* **108**, 201602 (2016).

[15] J. Repp, G. Meyer, S.M. Stojković, A. Gourdon, and C. Joachim, *Phys. Rev. Lett.* **94**, 26803 (2005).

[16] G. Binnig and H. Rohrer, Rev. Mod. Phys. **59**, 615 (1987).

[17] G. Binnig, H. Rohrer, C. Gerber, and E. Weibel, *Phys. Rev. Lett.* **50**, 120 (1983).

[18] O. Dulub, W. Hebenstreit, and U. Diebold, *Phys. Rev. Lett.* **84**, 3646 (2000).

[19] J.S. Villarrubia, *J Res Natl Inst Stand Technol* **102**, 102 (1997).

[20] L. Lichtenstein, C. Büchner, B. Yang, S. Shaikhutdinov, M. Heyde, M. Sierka, R. Włodarczyk, J. Sauer, and H.-J. Freund, *Angew. Chem. Int. Ed.* **51**, 404 (2012).

[21] L. Lichtenstein, M. Heyde, and H.-J. Freund, *J. Phys. Chem. C* **116**, 20426 (2012).

[22] E.I. Altman and U.D. Schwarz, *Adv. Mater. Interfaces* **1**, 1400108 (2014).

[23] P.Y. Huang, S. Kurasch, J.S. Alden, A. Shekhawat, A.A. Alemi, P.L. McEuen, J.P. Sethna, U. Kaiser, and D.A. Muller, *Science* **342**, 224 (2013).

[24] P.Y. Huang, S. Kurasch, A. Srivastava, V. Skakalova, J. Kotakoski, A.V. Krasheninnikov, R. Hovden, Q. Mao, J.C. Meyer, J. Smet, D.A. Muller, and U. Kaiser, *Nano Lett.* **12**, 1081 (2012).

[25] D. Loeffler, J.J. Uhlrich, M. Baron, B. Yang, X. Yu, L. Lichtenstein, L. Heinke, C. Büchner, M. Heyde, S. Shaikhutdinov, H.-J. Freund, R. Wlodarczyk, M. Sierka, and J. Sauer, *Phys. Rev. Lett.* **105**, 146104 (2010).

[26] L. Lichtenstein, C. Büchner, B. Yang, S. Shaikhutdinov, M. Heyde, M. Sierka, R. Włodarczyk, J. Sauer, and H.-J. Freund, *Angew. Chem. Int. Ed.* **51**, 404 (2012).

[27] J.F. Shackelford and L.P. Davila, *J. Non-Cryst. Solids* **356**, 2444 (2010).

[28] J.F. Shackelford and B.D. Brown, *J. Non-Cryst. Solids* **44**, 379 (1981).

[29] M. Heyde, G.H. Simon, and L. Lichtenstein, *Phys. Status Solidi B-Basic Solid State Phys.* **250**, 895 (2013).

[30] P.H. Gaskell and I.D. Tarrant, *Philos. Mag. Part B* **42**, 265 (1980).

[31] R.J. Bell and P. Dean, *Philos. Mag.* **25**, 1381 (1972).

[32] C. Büchner, L. Liu, S. Stuckenholz, K.M. Burson, L. Lichtenstein, M. Heyde, H.-J. Gao, and H.-J. Freund, *J. Non-Cryst. Solids* **435**, 40 (2016).

[33] S.D. Eder, K. Fladischer, S.R. Yeandel, A. Lelarge, S.C. Parker, E. Søndergård, and B. Holst, *Sci. Rep.* **5**, 14545 (2015).

[34] K.M. Burson, C. Büchner, M. Heyde, and H.J. Freund, *J. Phys. Condens. Matter* **29**, 035002 (2017).

[35] F. Wooten and D. Weaire, *J. Non-Cryst. Solids* **114**, 681 (1989).

[36] K.M. Burson, P. Schlexer, C. Büchner, L. Lichtenstein, M. Heyde, and H.-J. Freund, *J. Chem. Educ.* **92**, 1896 (2015).

[37] C. Büchner, P. Schlexer, L. Lichtenstein, S. Stuckenholz, M. Heyde, and H.-J. Freund, *Z. Phys. Chem.-Int. J. Res.* **228**, 587 (2014).

[38] L. Bragg and J. Nye, *Proc. R. Soc. Lond. Ser. -Math. Phys. Sci.* **190**, 474 (1947).

[39] A.K. Geim and I.V. Grigorieva, *Nature* **499**, 419 (2013).

[40] X. Yu, E. Emmez, Q. Pan, B. Yang, S. Pomp, W.E. Kaden, M. Sterrer, S. Shaikhutdinov, H.-J. Freund, I. Goikoetxea, R. Wlodarczyk, and J. Sauer, *Phys. Chem. Chem. Phys.* **18**, 3755 (2016).

[41] F. Ringleb, Y. Fujimori, H.-F. Wang, H. Ariga, E. Carrasco, M. Sterrer, H.-J. Freund, L. Giordano, G. Pacchioni, and J. Goniakowski, *J. Phys. Chem. C* **115**, 19328 (2011).

[42] F. Ringleb, M. Sterrer, and H.-J. Freund, *Appl. Catal. Gen.* **474**, 186 (2014).

[43] F.F. Abraham and I.P. Batra, *Surf. Sci. Lett.* **209**, L125 (1989).

[44] M. Osada and T. Sasaki, *Adv. Mater.* **24**, 210 (2012).

[45] E. Gao, B. Xie, and Z. Xu, *J. Appl. Phys.* **119**, 14301 (2016).

[46] L. Lichtenstein, M. Heyde, S. Ulrich, N. Nilius, and H.-J. Freund, *J. Phys.-Condens. Matter* **24**, 354010 (2012).

[47] C. Büchner, Z.-J. Wang, K.M. Burson, M.-G. Willinger, M. Heyde, R. Schlögl, and H.-J. Freund, *ACS Nano* **10**, 7982 (2016).